PREVIRIALIZATION

E. L. Łokas[1], R. Juszkiewicz[1,2], F. R. Bouchet[3] and E. Hivon[3]

[1] Copernicus Astronomical Center, Bartycka 18, 00-716 Warsaw, Poland
[2] Institute for Theoretical Physics, University of California,
Santa Barbara, California 93106-4030, USA
[3] Institut d'Astrophysique de Paris, 98 bis Bd Arago, 75014 Paris, France

E–mail: lokas@camk.edu.pl (ELŁ), roman@camk.edu.pl (RJ), bouchet@iap.fr (FRB),
hivon@iap.fr (EH)

ABSTRACT

We propose a method to solve the "previrialization" problem of whether the non-linear interactions between perturbations at different scales increase or decrease the rate of growth of structure. As a measure of this effect we calculate the weakly non-linear corrections to the variance of the probability distribution function of the density field. We assume Gaussian initial conditions and use perturbative expansions to calculate these corrections for scale–free initial power spectra. As a realistic example, we also compute the corrections for the spectrum proposed by Peacock & Dodds (1994). The calculations are performed for both a Gaussian and a top-hat smoothing of the evolved fields. We show that the effect of weakly non-linear interactions depends strongly on the spectral index; they increase the variance for the spectral index $n = -2$, but decrease it for $n \geq -1$. Finally, we compare our perturbative calculations to N–body simulations and a formula of a type proposed by Hamilton et al. (1991).

Subject headings: cosmology: theory – galaxies: clustering – galaxies: formation – large–scale structure of universe

Submitted to *ApJ*

1 Introduction

The "previrialization" hypothesis in studies of structure formation states that the nonradial motions in a developing mass concentration may slow down the collapse and therefore the formation of virialized objects. The possibility was first seriously considered by Davis & Peebles (1977) who mentioned two examples of application. The first is that of a protocluster collapsing along one axis while it is still expanding as a whole. The other concerns the production of internal kinetic energy through tidal interaction among neighboring protoclusters. The N–body experiments of Villumsen & Davis (1986) appear to reproduce these effects.

Peebles (1990) presented a numerical method for the description of a developing protocluster. Constructed explicitly as a slightly overdense region of randomly placed particles, the protocluster is then evolved back in time using the least action method. When the system is isolated the particle orbits trace back to the primeval density contrast which is found consistent with the spherical model. In the presence of neighboring clusters however, the test particles move in a more non–radial way increasing the primeval contrast. Although the spherical model predicts that the growth of the density contrast is faster than the linear approximation, the growth observed in the numerical action method is slower.

While Peebles (1990) considered the influence of larger scales on a forming protocluster which had no substructure, Evrard & Crone (1992) posed the question, whether small–scale structure affects the clustering on larger scales. Their N–body simulations supported the conclusion that the abundance of rich clusters finally formed was insensitive to the amount of small–scale power present in the initial conditions. The analysis, however, focused on the case with the initial power spectrum index $n = -1$ which, as we will show, is not the best chosen one to observe the effect of previrialization.

An independent and very powerful tool for the analysis of interactions between perturbations at different scales is the weakly non–linear perturbation theory (Peebles, 1980; Juszkiewicz 1981). Juszkiewicz, Sonoda & Barrow (1984) showed that non–linear gravitational effects result in the shortening of the characteristic scale of galaxy clustering and the interaction between long wavelength perturbations can be viewed as a source of perturbations of shorter wavelength.

There followed a number of studies devoted to calculations of weakly non–linear corrections to the power spectrum. Suto & Sasaki (1991) and Makino, Sasaki & Suto (1992) provided analytical formulas for the case of scale–free power–law power spectra. Jain & Bertschinger (1994) performed numerical calculations for the standard CDM spectrum and found that due to the non–linear mode coupling, characteristic non–linear masses grow less

slowly in time than the linear theory would predict. Baugh & Efstathiou (1994) checked perturbative calculations of the non–linear CDM spectrum against N–body simulations and found a significant transfer of power from larger to smaller scales.

As a measure of the "previrialization" effect we calculate the weakly non–linear corrections to the second moment (the variance) of the probability distribution of the cosmic density field. As pointed out by Suto & Sasaki (1991) and Makino et al. (1992) the results are expected to depend on the assumed form of power spectrum of the primordial fluctuations and may be useful in obtaining the amplitude of the spectrum needed to produce a given class of objects such as galaxies or clusters of galaxies that we observe today.

This paper is organized as follows. In section 2, we summarize the formalism of weakly non–linear perturbation theory and calculate the second order contributions to the variance. We use Gaussian initial conditions and perform the calculations for scale–free power–law spectra and the spectrum of Peacock & Dodds (1994). The results and discussion are given in Section 3, where we compare our calculations to the N–body simulations and a formula of a type proposed by Hamilton, Kumar & Matthews (1991).

2 Perturbation theory

We assume a model universe with vanishing cosmological constant and arbitrary density parameter Ω. The content of the universe is supposed to behave as pressureless fluid which undergoes gravitational evolution described by the usual Newtonian equations. The cosmic density field is characterized by the density contrast $\delta = \delta(\mathbf{x}, t) = \delta\rho/\rho_b$, where $\mathbf{x}$ is the Eulerian comoving coordinate and ρ_b denotes the background density.

The perturbative expansion of the density contrast around the background solution $\delta = 0$ is

$$\delta = \delta_1 + \delta_2 + \delta_3 + \cdots \tag{1}$$

where $\delta_n = \mathcal{O}(\delta_1^n)$, δ_1 being the linear theory solution. The n–th order solutions are obtained from equations describing the Newtonian evolution using the solutions of the $(n-1)$–th order of density and velocity fields as source terms (see Fry 1984; Goroff et al. 1986).

In the Einstein–de Sitter universe the scale factor $a \propto t^{2/3}$ and the background density $\rho_b = 3\dot{a}^2/8\pi G a^2 = 1/6\pi G t^2$. The time dependence of the n–th order follows

$$\delta_n(\mathbf{x}, t) = [D(t)]^n \delta_n(\mathbf{x}) \tag{2}$$

where $D(t) \propto a(t)$ and we consider only the mode growing in time. For an arbitrary

cosmological model, however, the time dependences of different orders should be considered independently. Fortunately for a wide range of Ω the solutions for the density contrast are very weakly dependent on Ω and the E–dS case provides a good approximation (Bouchet et al. 1992, 1995; Catelan et al. 1995).

All of the following calculations are much simpler if they are performed in Fourier space. For the first order of the density contrast field we have

$$\delta_1(\mathbf{k},t) = D(t)\int \mathrm{d}^3x\ \delta_1(\mathbf{x})\mathrm{e}^{-\mathrm{i}\mathbf{k}\cdot\mathbf{x}} \tag{3}$$

and the inverse Fourier transform is

$$\delta_1(\mathbf{x},t) = D(t)(2\pi)^{-3}\int \mathrm{d}^3k\ \delta_1(\mathbf{k})\mathrm{e}^{\mathrm{i}\mathbf{k}\cdot\mathbf{x}}. \tag{4}$$

For the following calculation only second and third order solutions for the density contrast are needed, and we give them here in the Fourier representation (e.g. Goroff et al. 1986).

$$\delta_2(\mathbf{k},t) = D^2(t)\frac{1}{(2\pi)^3}\int \mathrm{d}^3p\int \mathrm{d}^3q\ \delta^3(\mathbf{p}+\mathbf{q}-\mathbf{k})\delta_1(\mathbf{p})\delta_1(\mathbf{q})P_2^{(s)}(\mathbf{p},\mathbf{q}) \tag{5}$$

$$\delta_3(\mathbf{k},t) = D^3(t)\frac{1}{(2\pi)^6}\int \mathrm{d}^3p\int \mathrm{d}^3q\int \mathrm{d}^3r\ \delta^3(\mathbf{p}+\mathbf{q}+\mathbf{r}-\mathbf{k})\delta_1(\mathbf{p})\delta_1(\mathbf{q})\delta_1(\mathbf{r})P_3^{(s)}(\mathbf{p},\mathbf{q},\mathbf{r}). \tag{6}$$

The symmetrized kernels are of the form

$$P_2^{(s)}(\mathbf{p},\mathbf{q}) = \frac{1}{14}J(\mathbf{p}+\mathbf{q},\mathbf{p},\mathbf{q}) \tag{7}$$

$$\begin{aligned} P_3^{(s)}(\mathbf{p},\mathbf{q},\mathbf{r}) = \quad & A\,[\quad H(\mathbf{p}+\mathbf{q}+\mathbf{r},\mathbf{p})J(\mathbf{q}+\mathbf{r},\mathbf{q},\mathbf{r}) + \\ & +\quad H(\mathbf{p}+\mathbf{q}+\mathbf{r},\mathbf{q}+\mathbf{r})\,L(\mathbf{q}+\mathbf{r},\mathbf{q},\mathbf{r})] + \\ & +B\quad F(\mathbf{p}+\mathbf{q}+\mathbf{r},\mathbf{p},\mathbf{q}+\mathbf{r})L(\mathbf{q}+\mathbf{r},\mathbf{q},\mathbf{r}) + \\ & +\quad \begin{pmatrix} \mathbf{p}\to\mathbf{q} \\ \mathbf{q}\to\mathbf{r} \\ \mathbf{r}\to\mathbf{p} \end{pmatrix} + \begin{pmatrix} \mathbf{p}\to\mathbf{r} \\ \mathbf{q}\to\mathbf{p} \\ \mathbf{r}\to\mathbf{q} \end{pmatrix} \end{aligned} \tag{8}$$

where $A = 1/108$ and $B = 1/189$. In the expression above the notation follows that of Makino et al. (1992) i.e.

$$H(\mathbf{p},\mathbf{q}) = \frac{\mathbf{p}\cdot\mathbf{q}}{q^2} \tag{9}$$

$$F(\mathbf{p}+\mathbf{q},\mathbf{p},\mathbf{q}) = \frac{1}{2}\frac{|\mathbf{p}+\mathbf{q}|^2\mathbf{p}\cdot\mathbf{q}}{p^2q^2} \tag{10}$$

$$J(\mathbf{p}+\mathbf{q},\mathbf{p},\mathbf{q}) = 4\frac{(\mathbf{p}\cdot\mathbf{q})^{\mathbf{2}}}{p^2q^2} + 7\frac{p^2+q^2}{p^2q^2}\mathbf{p}\cdot\mathbf{q} + 10 \tag{11}$$

$$L(\mathbf{p}+\mathbf{q},\mathbf{p},\mathbf{q}) = 8\frac{(\mathbf{p}\cdot\mathbf{q})^{\mathbf{2}}}{p^2q^2} + 7\frac{p^2+q^2}{p^2q^2}\mathbf{p}\cdot\mathbf{q} + 6. \tag{12}$$

The smoothing of the fields is introduced by the convolution of the density and the filtering function

$$\delta_R(\mathbf{x},t) = \int \mathrm{d}^3 y \delta(\mathbf{y},t) W_R(|\mathbf{x}-\mathbf{y}|) \tag{13}$$

where the window function is normalized so that $\int \mathrm{d}^3 x W(x) = 1$. We perform our calculations for two types of the window functions, a Gaussian and a top–hat with Fourier representations respectively

$$W_G(pR) = \mathrm{e}^{-p^2R^2/2} \tag{14}$$

and

$$W_{TH}(pR) = 3\sqrt{\frac{\pi}{2}}(pR)^{-\frac{3}{2}} J_{\frac{3}{2}}(pR) \tag{15}$$

where $J_{\frac{3}{2}}$ is a Bessel function

$$J_{\frac{3}{2}}(pR) = \sqrt{\frac{2}{\pi pR}}\left(\frac{\sin(pR)}{pR} - \cos(pR)\right). \tag{16}$$

We assume a Gaussian distribution for δ_1 in equation (1) and define

$$\sigma^2 = \langle \delta_1^2 \rangle = D^2(t) \int \frac{\mathrm{d}^3 k}{(2\pi)^3} P(k) W^2(kR) \tag{17}$$

as the linear variance of the density field. We need $\sigma < 1$ for the perturbative expansion to be valid. The statistical properties of δ_1 and the next terms in the perturbative series (1) are fully determined, in the case of Gaussian models, by the power spectrum $P(k)$, defined as the Fourier transform of the two–point correlation function, which obeys the relation

$$\langle \delta(\mathbf{k}) \delta(\mathbf{p}) \rangle = (2\pi)^3 \delta^3(\mathbf{k}+\mathbf{p}) P(\mathbf{k}) \tag{18}$$

where **k, p** are comoving wavevectors.

First we consider initial power spectra with a power–law form

$$P(k) = Ck^n, \quad -3 \leq n \leq 1 \tag{19}$$

where C is a normalization constant. With this assumption the variance given by equation (17) becomes for the Gaussian filter

$$\sigma_G^2 = CD^2(t) \frac{\Gamma(\frac{n+3}{2})}{(2\pi)^2 R^{n+3}}, \tag{20}$$

and for the top–hat we obtain

$$\sigma_{TH}^2 = CD^2(t) \frac{9\Gamma(\frac{n+3}{2})\Gamma(\frac{1-n}{2})}{8\pi^{\frac{3}{2}} R^{n+3} \Gamma(1-\frac{n}{2})\Gamma(\frac{5-n}{2})} \tag{21}$$

which is divergent for $n = 1$.

Following the perturbative expansion (1) we have for the second moment of the density field up to the terms on the order of σ^4

$$\langle \delta^2 \rangle = \langle \delta_1^2 \rangle + \langle \delta_2^2 \rangle + 2\langle \delta_1 \delta_3 \rangle + \mathcal{O}(\sigma^6). \tag{22}$$

The first term is the linear variance given by equation (17) and the two other terms take into account the non–linear corrections. It turns out to be convenient to calculate the first non–linear corrections in a normalized form, i.e. divided by σ^4. Indeed, provided the integrals are convergent, for the scale–free power–law spectra, these ratios should be dimensionless numbers, independent of scale, as in the case of the higher moments (e.g. the skewness and the kurtosis) of the fields. By using the second and third order solutions (5) and (6) smoothed with any window function we obtain

$$I_{22} = \frac{\langle \delta_2^2 \rangle}{\sigma^4} = \frac{D^4(t)}{98(2\pi)^6 R^{2(n+3)} \sigma^4} \int \mathrm{d}^3 p \int \mathrm{d}^3 q \; P(p) P(q) W^2(|\mathbf{p}+\mathbf{q}|) \; J^2(\mathbf{p}+\mathbf{q}, \mathbf{p}, \mathbf{q}) \tag{23}$$

$$\begin{aligned} I_{13} = 2\frac{\langle \delta_1 \delta_3 \rangle}{\sigma^4} &= \frac{6D^4(t)}{(2\pi)^6 R^{2(n+3)} \sigma^4} \int \mathrm{d}^3 p \int \mathrm{d}^3 q \; P(p) P(q) W^2(q) \\ &\times \{ \; A \, [\; H(\mathbf{q}, -\mathbf{p}) \; J(\mathbf{p}+\mathbf{q}, \mathbf{p}, \mathbf{q}) \\ &\qquad + H(\mathbf{q}, \mathbf{p}+\mathbf{q}) \; L(\mathbf{p}+\mathbf{q}, \mathbf{p}, \mathbf{q})] \\ &\qquad - B \; F(\mathbf{q}, -\mathbf{p}, \mathbf{p}+\mathbf{q}) \; L(\mathbf{p}+\mathbf{q}, \mathbf{p}, \mathbf{q})\} + \begin{pmatrix} \mathbf{p} \to \mathbf{q} \\ \mathbf{q} \to \mathbf{p} \end{pmatrix} \end{aligned} \tag{24}$$

where the last term in brackets means that similar expression with $\mathbf{p}$ and $\mathbf{q}$ interchanged should be added if the symmetry in $\mathbf{p}$ and $\mathbf{q}$ is to be maintained. The integration with respect to angular variables is straightforward if spherical coordinates are used. In the case of the Gaussian filter the result for I_{22} is rather lengthy so we do not give it here, for I_{13} it is more concise

$$\begin{aligned} I_{13} &= \frac{1}{252\Gamma^2(\frac{n+3}{2})} \int \mathrm{d}p \int \mathrm{d}q \; P(p) P(q) \mathrm{e}^{-p^2} \left[12\frac{p^6}{q^2} - 158p^4 + 100p^2q^2 - 42q^4 + \right. \\ &+ \left. \frac{3}{pq^3}(q^2-p^2)^3(7p^2+2q^2) \ln \frac{p+q}{|q-p|} \right] + \begin{pmatrix} \mathbf{p} \to \mathbf{q} \\ \mathbf{q} \to \mathbf{p} \end{pmatrix}. \end{aligned} \tag{25}$$

We see that the expression is similar to the result of angular integration obtained by Makino et al. (1992) when calculating the first non–linear corrections to the power spectrum. Indeed, our approach is strictly equivalent to calculating the variance (17) with their weakly non–linear spectrum $P(k) = P_{11}(k) + P_{22}(k) + 2P_{13}(k)$, where the last two terms represent the non–linear corrections, instead of the linear part $P_{11}(k)$ of the form given by equation (19).

The input from I_{22} is always positive and from I_{13} negative, therefore we may interpret their values at some scale respectively as the additional power coming in from other wavelengths and the second as the power that is lost and taken over by other wavelengths.

Both I_{22} and I_{13} diverge individually in the limit of $p \to 0$ and $q \to 0$ if $n \leq -1$. Fortunately for the whole range $-3 \leq n \leq 1$ their leading terms cancel each other in this limit. In the opposing limit of $p \to \infty$ and $q \to \infty$ divergencies are present for I_{22} if $n > \frac{1}{2}$ and for I_{13} if $n > -1$. Therefore if we want to calculate the sum of both terms for $n > -1$ we need to introduce a cut–off in the initial power spectrum at large wave-numbers

$$P(k) = \begin{cases} Ck^n & \text{for } 0 < k < k_c \\ 0 & \text{for } k > k_c. \end{cases} \tag{26}$$

An equivalent way to introduce the cut–off is to smooth the power spectrum with a Gaussian

$$P(k) = Ck^n \mathrm{e}^{-k^2 r^2} \tag{27}$$

where the small smoothing length r should correspond e.g. to the small scale cut–off of the initial spectra in the N–body simulations.

3 Results and discussion

3.1 Scale–free power spectra

In the case of no smoothing both the corrections and σ^4 diverge but their ratio remains finite. By numerically integrating I_{22} and I_{13} with $W(pR) = 1$ we obtain

$$\frac{< \delta_2^2 > +2 < \delta_1 \delta_3 >}{\sigma^4} = 1.83. \tag{28}$$

This value is very weakly *dependent* on n (contrary to the lowest order values of normalized cumulants). It decreases slightly with growing spectral index n, but differences in the range $-3 \leq n \leq 1$ are smaller than 1 %. Therefore we may approximate the weakly non–linear $< \delta^2 >$ as

$$\sigma^2_{wnl} = \sigma^2 + 1.83\sigma^4. \tag{29}$$

Figure 1 shows the results of the calculation of the weakly non–linear corrections $< \delta_2^2 > +2 < \delta_1 \delta_3 >$ divided by σ_G^4 (eq. [20]) for a Gaussian filter and different power spectra. The corrections are shown for different values of the variable $k_c R$, where k_c is the cut–off of the initial power spectrum, and R is the scale of the final smoothing. We see that the

integrals are convergent only when $n = -2$. In that case, when $k_c \to \infty$, that is in the no cut–off limit, we obtain

$$\frac{< \delta_2^2 > +2 < \delta_1 \delta_3 >}{\sigma_G^4} = 0.86 \tag{30}$$

and

$$\sigma_{wnl}^2 = \sigma^2 + 0.86\sigma^4. \tag{31}$$

This applies in the present case where $\sigma^2 = \sigma_G^2$. For higher spectral indices n, the integrals do not converge and the cut–off introduces the dependence of the results on R.

A similar behaviour is observed for the top–hat smoothing. Indeed a relation like equation (31) holds for $n = -2$, but the corresponding numerical value is extremely difficult to determine exactly. This comes from the oscillatory behaviour of the top-hat filter in Fourier space. We tried to avoid this difficulty by approximating the top–hat filter by a Gaussian

$$W_{TH}(pR) \simeq \mathrm{e}^{-p^2R^2/9} \tag{32}$$

which is accurate to within few percent in the whole range of integration. The resulting numerical value of the weakly non–linear correction (30) is then the same (up to the given accuracy) as in the Gaussian case.

3.1.1 Comparison with N–body simulations

To compare predictions of perturbation theory to the N–body results in the case of spectral indices $n = -1, n = 0$ and $n = +1$ we use the simulations made by David Weinberg that were used to check the perturbative calculation of skewness and kurtosis (Juszkiewicz et al. 1995, Łokas et al. 1995). All the simulations used a 200^3 force mesh and 100^3 particles (except for n=+1 ones which had 200^3 particles). The moments of the evolved density field were computed for Gaussian smoothing lengths $L/50$, $L/25$ and $L/12.5$, $L = 100$ cells being the size of the simulation box.

Figure 2 compares the N–body results to the perturbative calculations. Open symbols show the ratios of the N–body non–linear variance to its linear counterpart calculated from equation (20) using the normalization of the initial power spectra (i.e. $\sigma = 1$ for the final expansion factor $a = 1$ and smoothing scale $L/50$). Circles, triangles and squares correspond to the shortest, medium and largest smoothing scale respectively. The error bars of the results (not plotted) coming from statistical averaging over eight independent simulations are large enough (especially in the $n = -1$ case where the points are most scattered) so that the results do not contradict self–similarity.

A direct, quantitative comparison between the perturbative and N–body results for $n > -2$ is restrained by the difficulty of determining the real small scale cut–off in the initial power spectra of the simulations. The degree of self–similarity displayed by the N–body results would indicate that the cut–off scale is very small. We performed the perturbative calculations of the weakly non–linear corrections to the variance for the spectrum (27) with a Gaussian cut–off at different wavelengths r: r_{Ny}, $r_{Ny}/2$ and $r_{Ny}/4$, where r_{Ny} is the scale corresponding to the Nyquist frequency. (The Nyquist scale is $L/50$ for $n = -1$ and $n = 0$ simulations and $L/100$ in the case of $n = +1$.) The choice of a cut–off scale r obviously breaks the self–similarity of the results. We showed in Figure 2 only the results of perturbative calculation corresponding to the medium final smoothing radius $L/25$ (filled triangles). We find that the perturbative results match the N–body best when we assume the cut–off scales $r = r_{Ny}/4$ for $n = -1$, $r = r_{Ny}/2$ for $n = 0$ and $r = r_{Ny}$ for $n = +1$.

In the $n = -2$ case, we performed a new simulation with 256^3 particles (about 17 million) using a PM code (Bouchet, Adam & Pellat 1985, Moutarde et al. 1991) with 256^3 cells. The initial conditions were imprinted using Zeldovich approximation on a "glass"-like particle distribution (White 1994), with a power equal to 1/25 of the shot noise level at the Nyquist frequency of the particle grid. This "glass" distribution was obtained by N–body simulation in an expanding universe with a *repulsive* gravitation, starting from a random initial distribution. After a high enough expansion (about 10^6 in our case), particles settle down in a quasi–equilibrium state. This state shows a very uniform particle load without any anisotropy or discernible order down to very small scales. This homogeneity allows a very accurate study of structure formation, in high density region, as well as in voids. The variance of the evolved density field was computed on the discrete distribution of a 64^3 particle sub–sample convolved with a spherical top–hat of radius R. Poisson noise associated to discreteness effects has been removed from measured variances.

Figure 3 compares the perturbative predictions and the N–body results for $n = -2$. Open symbols show the ratios of the non-linear variances to the linear ones, at different expansion factors and at 8 scales, starting from $R = 10^{-2.2}$ times the box size, and spaced by 0.2 in log. The linear variances were calculated according to equation (21) and the perturbative weakly non–linear approximations to the non-linear ones (filled symbols in Figure 3) using equation (31). The N–body results closely follow theoretical predictions and obey a self-similar evolution, apart from the largest scale measurements (with $R = 10^{-0.8}$ times the box size). These deviations are likely to be due to the effect of the missing waves at scales larger than the numerical box. The absence of these long waves can also explain the slight offset of the numerical results vs. the theory, because according to Figure 1, for $n = -2$, the correction to linear theory for variance is actually quite sensitive to long waves contribution. We have calculated the perturbative corrections with a cut–off at low

wavevectors corresponding to the size of the box for a few points in Figure 3 and found that introducing this cut–off decreases both the linear variance σ^2 and the weakly non–linear approximation of $< \delta^2 >$ but their ratio also is decreased. Therefore the effect of such a cut–off is generally to decrease the perturbative values in Figure 3 so that they are much closer to the N–body results.

Both the perturbation theory and N–body experiments seem to support the statement that the weakly non–linear evolution is likely to increase the value of $< \delta^2 >$ compared to the linear case for $n = -2$ and decrease it for $n \geq -1$, with the effect becoming more prominent for higher spectral indices.

3.1.2 Comparison with Hamilton–type formula

Hamilton et al. (1991) proposed a general formula relating the linear two–point correlation function of arbitrary shape and its strongly non–linear counterpart. While physically motivated in its limits, the overall functional shape of the relation was modeled using N–body simulations of scale–free initial power spectra with $\Omega = 1$. A similar formula for power spectra was obtained by Peacock & Dodds (1994) and recently refined to take into account the dependence on the spectral index of the spectrum by Mo, Jain & White (1995). We will use this n–dependent formula to calculate the non–linear variance and compare the result to the linear prediction as was done in the case of perturbative approximation and N–body simulations.

The ansatz for the relation between the linear power spectrum ($\Delta_L(k_0) = 4\pi k_0^3 P(k_0)$) and the non–linear (evolved) one ($\Delta_E(k) = 4\pi k^3 P(k)$) is

$$\frac{\Delta_E(k)}{B(n)} = \Phi\left[\frac{\Delta_L(k_0)}{B(n)}\right] \tag{33}$$

where the wavevectors k and k_0 are related by

$$k = [1 + \Delta_E(k)]^{1/3} k_0 \tag{34}$$

and $B(n)$ is a constant depending on the power spectrum index n. The values of $B(n)$ are 1.64, 1, 0.54 and 0.24 for $n = +1$, $n = 0$, $n = -1$ and $n = -2$ respectively. We use the fitting formula of Mo et al. (1995)

$$\Phi(x) = x\left(\frac{1 + 2x^2 - 0.6x^3 - 1.5x^{7/2} + x^4}{1 + 0.0037x^3}\right)^{1/2} \tag{35}$$

to calculate the non–linear power spectrum Δ_E at specified values of k_0. Then, using equation (34) we find the value of k corresponding to each of pairs $[k_0, \Delta_E(k_0)]$. The list of

points $[k, \Delta_E(k)]$ is then fitted numerically by the linear power spectrum plus polynomial terms of higher order. This fitted shape of the non–linear power spectrum $\Delta_E(k)$ is then used to calculate the non–linear variance $< \delta^2 >$. For simplicity we use a filter function in the form of a top–hat in Fourier space (that is we cut off the integration at some wavenumber k_c), the effect of which should be close to the effect of a Gaussian filter with the smoothing scale corresponding to k_c. The comparison of the results with the linear variance, σ^2, is shown in Figure 4. Given the numerous approximations applied in the calculations, the agreement between the results thus obtained with those of perturbative calculations and N–body simulations (Figures 2 and 3) is rather impressive.

3.2 The Peacock–Dodds spectrum

In the case of a realistic power-spectrum, which has different slopes for different ranges of the wave–number, the non–linear evolution will introduce different effects depending on the local slope of the spectrum. As an example of such a spectrum we consider the following

$$\Delta(k) = \frac{(\frac{k}{k_0})^\alpha}{1 + (\frac{k}{k_c})^{\alpha-\beta}} \tag{36}$$

where $\Delta(k) = 4\pi k^3 P(k)/(2\pi)^3$. The parameters given by Peacock & Dodds (1994),

$$\begin{aligned} k_0 &= 0.29 \pm 0.01 \ h \ \mathrm{Mpc}^{-1} \\ k_c &= 0.039 \pm 0.002 \ h \ \mathrm{Mpc}^{-1} \\ \alpha &= 1.50 \pm 0.03 \\ \beta &= 4.0 \pm 0.5, \end{aligned} \tag{37}$$

were fitted to best match the data obtained from eight independent surveys. The reconstruction of this linear spectrum involved accounting for non–linear evolution as well as redshift space distortions. If we accept the most probable value $\alpha - \beta = -2.5$ we may rewrite the spectrum in the following way

$$P(k) = \frac{Ck}{1 + (\frac{k}{k_c})^n} \tag{38}$$

with $C = 2\pi^2 k_0^{-1.5} k_c^{-2.5}$ and $n = 2.5$. The spectrum of this kind was first considered by Peacock (1991) who quotes k_c in the range $[0.015, 0.025]$ h Mpc^{-1} and $n = 2.4$.

The linear variance of the density contrast averaged over spheres of radius R is calculated according to equation (17)

$$\sigma_R^2 = \frac{9\pi}{2k_0^{1.5} k_c^{2.5} R^4} \int_0^\infty \frac{\mathrm{d}k}{1 + (\frac{k}{k_c R})^{2.5}} J_{3/2}^2(k) \tag{39}$$

which is easily integrable numerically. Assuming the smoothing scale $R = 8\ h^{-1}$ Mpc we obtain

$$\sigma_8 = 0.69. \tag{40}$$

The weakly non–linear corrections are calculated using equations (23) and (24) and the approximate top–hat filter (32). The convergence of the integrals is now ensured because for $k \to \infty$ the power spectrum (38) approaches $C/k^{1.5}$. The calculation of the corrections must however be done for every considered smoothing scale independently as the spectrum is not scale–free. At $R = 8\ h^{-1}$ Mpc we find

$$\frac{(< \delta_2^2 > +2 < \delta_1 \delta_3 >)_8}{\sigma_8^4} = 0.15 \tag{41}$$

and the value of σ_8 taking into account the weakly non–linear corrections is

$$\sigma_{8,wnl} = 0.72 \tag{42}$$

which is less than 4 % above the linear value. This result is consistent with what we have shown above for the scale–free power spectra. At the scale of 8 h^{-1} Mpc the spectrum has index close to -1 or slightly below this value. For such spectral indices we expect the weakly non–linear variance to be equal to or slightly above the linear value.

One may ask how the result will change if we apply different values of the fitting parameters (37). The one of least accuracy is the β parameter. However, even if we vary it in the whole quoted range the behaviour of the power spectrum at large wave–numbers will not change and will still have the $C/k^{1.5}$ slope. It is only for this part of the power spectrum that the values of σ are significant enough for the weakly non–linear corrections to become relevant. These arguments are confirmed by the numerical integration of the corrections with $\beta = 3.5$ and $\beta = 4.5$. This uncertainty in β translates into the value of (41): 0.15 ± 0.02. The only more significant changes that the parameter β may introduce affect the low k part of the spectrum where σ values are small and perturbative corrections are negligible.

We may also think of varying the parameter k_c which corresponds roughly to the point of the break in the power spectrum. Higher k_c allow more power of the spectral index $n = 1$ and $n = 0$ that could slightly increase the power spectrum index at the weakly non–linear scale and therefore decrease the correction (41). However all the parameters (37) of the fitted spectrum except for β are quite exactly determined so that the possible changes of the value (41) due to the uncertainties of these parameters are negligible. Of course we must remember that the values (37) were obtained via a number of approximations among which the most significant are probably the procedure applied to unify the data coming from different surveys and the method to account for the non–linear evolution which is not expected to work equally well for different parts of the power spectrum.

3.3 Concluding remarks

We have computed the first non–linear corrections to the variance of a density field undergoing gravitational instability. The results are confirmed by numerical simulations, and agree with the ansatz of Hamilton et al. (1991), as modified by Mo et al. (1995). There is indeed a previrialization effect, as conjectured by Peebles. The effect depends on the initial power spectrum considered, and essentially vanishes for power spectrum indices close to one, in agreement with the results of the simulations by Evrard and Crone (1992).

For scale–free power spectra the difference between the linear and weakly non–linear approximation for the variance can be as high as 100% as in the case of the spectral index $n = -2$. For the realistic power spectrum of a class considered by Peacock & Dodds (1994) however, we have found that the correction induced by weakly non-linear effects on σ_8 is very weak. This is purely by chance: the effective index of the realistic spectrum happens to be close to $n = -1$ for which, as we have seen, the non–linear correction changes sign and is close to zero.

Our results are in agreement with previous attempts to account for the non–linear interaction between perturbations at different scales. Using the fluid model for the evolution of structure Peebles (1987) found that for the initial power spectrum of index $n = 0$ (and some small scale cut–off) the smoothed standard deviation of the evolved field is decreased by non–linear interactions (e.g. $\sigma = 0.35$ is 15% below the linear extrapolation). Weinberg & Cole (1992) performed a series of N–body simulations with Gaussian initial conditions and scale–free initial power spectra normalized so that the evolved $\sigma_8 = 1$. For the power spectrum index $n = -1$ they found that σ_8 grows at almost exactly the rate predicted by linear theory, while for $n = 0$ the required linear σ_8 was larger than the evolved value and for $n = -2$ smaller. Jain & Bertschinger (1994) found that for CDM spectrum normalized so that linear $\sigma_8 = 1$ the second–order effects increase σ_8 by 10%.

Such dependence of the effect of non–linear interactions on the shape of the initial spectrum of fluctuations is consistent with the physical picture associated with the power spectrum itself. Let us imagine a slightly overdense region contained inside a surface of radius r. If the power spectrum of density fluctuations has a slope of $n = -2$ than the behaviour of the matter inside the region will be dominated by the perturbations at large scales, where there is a lot of power, and the effect of this interaction should be global, similar for different parts of the protocluster. For large indices e.g. $n = +1$ the behaviour of the overdense region would be dominated by the small scale granulation inside it that would cause random motions of different parts of the protocluster. This is likely to slow down the collapse of the region. For this type of spectra we have found the weakly non–

linear corrections to be divergent. The reason for this might be that the presence of large amounts of power at small scales would result in a kind of pressure that is not properly described by the pressureless fluid approximation on which the perturbation theory applied here was based.

Another simple argument suggesting similar effect of the power spectrum shape on the rate of collapse is the calculation of the peculiar gravitational acceleration produced by the overdense region on scale r (Peebles & Groth 1976; Vittorio & Juszkiewicz 1987). For scale–free power spectra the acceleration is proportional to $r^{-(n+1)/2}$, which diverges at large r if $n < -1$. The value $n = -1$ marks the transition between the power spectra for which the acceleration grows with r ($n > -1$) and decreases with r ($n < -1$). These simple arguments seem to support the description of the evolution of perturbations obtained within the framework of weakly non–linear perturbation theory.

Acknowledgements

We wish to thank Michał Chodorowski and Paolo Catelan for discussions and comments that helped to improve the presentation of results. We are greatful to David Weinberg for the use of his N–body simulations. The computational means (CRAY-98) have been made available to us thanks to the scientific council of the Institut du Développement et des Resources en Informatique Scientifique (IDRIS). ELŁ and RJ thank Alain Omont for his hospitality at Institut d'Astrophysique de Paris where part of this work was done. This research has been supported in part by the French Ministry of Research and Technology within the programme RFR, the Polish State Committee for Scientific Research grant No. 2P30401607 and the National Science Foundation grant No. PHY94-07194.

References

Baugh, C. M. & Efstathiou, G. 1994, MNRAS, 270, 183

Bouchet, F. R., Adam, J.-C., & Pellat, R. 1985, A&A, 144, 413

Bouchet, F. R., Juszkiewicz, R., Colombi, S & Pellat, R. 1992, ApJ, 394, L5

Bouchet, F. R., Colombi, S., Hivon, E. & Juszkiewicz, R. 1995, A&A, 296, 575

Catelan, P., Lucchin, F., Matarrese, S. & Moscardini, L. 1995, MNRAS, 276, 39

Davis, M. & Peebles, P. J. E. 1977, ApJS, 34, 425

Evrard, A. E. & Crone, M. M. 1992, ApJ, 394, L1

Fry, J. N. 1984, ApJ, 279, 499

Goroff, M. H., Grinstein, B., Rey, S.-J. & Wise, M. B. 1986, ApJ, 311, 6

Hamilton, A. J. S., Kumar, P., Lu, E. & Matthews, A. 1991, ApJ, 374, L1

Jain, B. & Bertschinger, E. 1994, ApJ, 431, 495

Juszkiewicz, R. 1981, MNRAS, 197, 931

Juszkiewicz, R., Sonoda, D. H. & Barrow, J. D. 1984, MNRAS, 209, 139

Łokas, E. L., Juszkiewicz, R., Weinberg, D. H. & Bouchet, F. R. 1995, MNRAS, 274, 730

Makino, N., Sasaki, M. & Suto, Y. 1992, Phys. Rev. D, 46, 585

Mo, H. J., Jain, B & White, S. D. M. 1995, MNRAS, submitted

Moutarde, F., Alimi, J.-M., Bouchet, F. R., & Pellat, R., ApJ, 382, 377

Peacock, J. A. 1991, MNRAS, 253, 1P

Peacock, J. A. & Dodds, S. J. 1994, MNRAS, 267, 1020

Peebles, P. J. E. 1980, The Large–scale Structure of the Universe, (Princeton: Princeton University Press)

Peebles, P. J. E. 1987, ApJ, 317, 576

Peebles, P. J. E. 1990, ApJ, 365, 27

Peebles, P. J. E. & Groth, E. J. 1976, A&A, 53, 131

Suto, Y. & Sasaki, M. 1991, Phys. Rev. Lett., 66, 264

Villumsen, J. V. & Davis, M. 1986, ApJ, 308, 499

Vittorio, N & Juszkiewicz, R. 1987, in: Proceedings of the Santa Cruz Summer Workshop in Astronomy and Astrophysics "Nearly Normal Galaxies", ed. S. M. Faber, (New York: Springer-Verlag), 451

Weinberg, D. H. & Cole, S. 1992, MNRAS, 259, 652

White, S. D. M. 1994, Les Houches Lectures, August 1993, `astro-ph/9410043`

Figure captions

Figure 1 Weakly non-linear corrections to the variance $< \delta_2^2 > + < \delta_1 \delta_3 >$ (eqs. [23]–[24]) divided by σ_G^4 (eq. [20]) for Gaussian filter and different scale–free power spectra. Symbols show the results of numerical integration up to different values of $k_c R$, where k_c is the cut–off wavenumber and R is the scale of the final smoothing. Only for $n = -2$ the integration converges to 0.86.

Figure 2 The ratio of the non-linear ($< \delta^2 >$) and linear (σ^2) variance as a function of σ^2 for different initial power spectra. Open symbols correspond to the results of N–body simulations with Gaussian smoothing lengths of $L/12.5$ (squares), $L/25$ (triangles) and $L/50$ (circles), where L is the size of the simulation box. Filled triangles show the results of perturbative calculations with final smoothing radius $L/25$ and the small scale cut–off $r_{Ny}/4$ for $n = -1$, $r_{Ny}/2$ for $n = 0$ and r_{Ny} for $n = +1$.

Figure 3 The comparison of the perturbative vs. N–body results for the power spectrum of index $n = -2$. Open symbols show the ratio of the non–linear ($< \delta^2 >$) and linear (σ^2) variance measured in N–body experiment at different expansion factors and eight final smoothing scales starting from $R = 10^{-2.2}$ times the size of the simulation box and spaced by 0.2 in log. The corresponding perturbative results (filled symbols) were calculated assuming the normalization of the simulated initial spectrum and using equations (30)–(31).

Figure 4 The ratio of the non-linear ($< \delta^2 >$) and linear (σ^2) variance as a function of σ^2 for different initial scale–free power spectra. The non–linear variance was obtained from the non–linear power spectrum given by a Hamilton–type ansatz (eqs. [33]–[35]). Both linear and non–linear values were calculated using a top–hat filter in Fourier space.

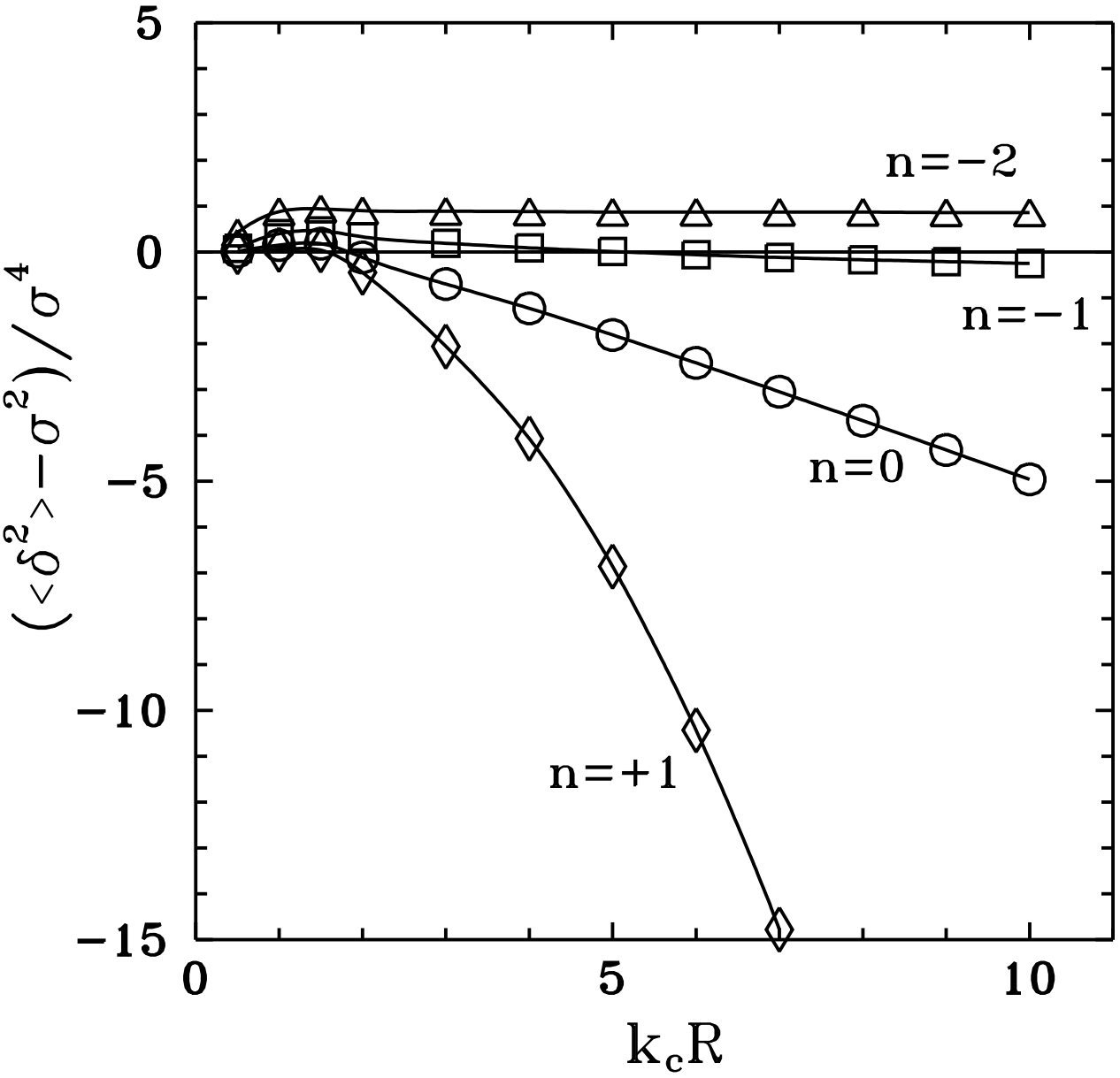

Figure 1

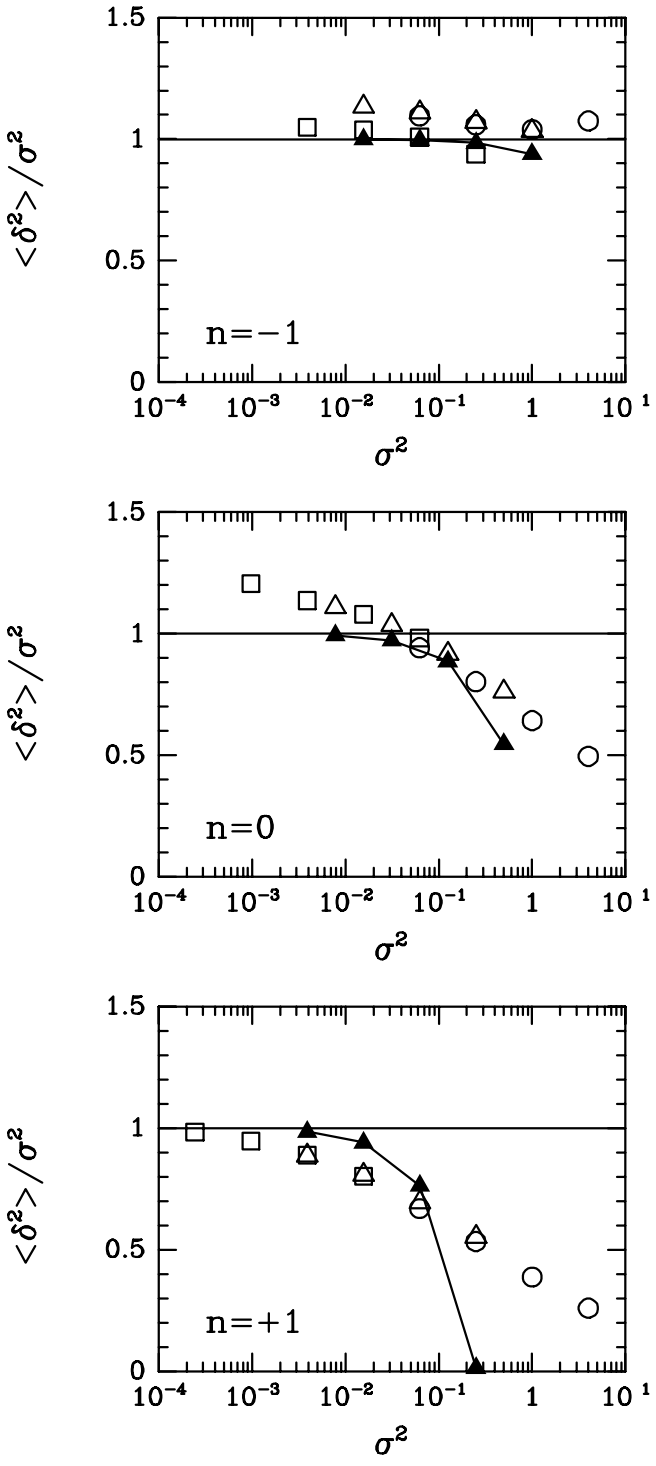

Figure 2

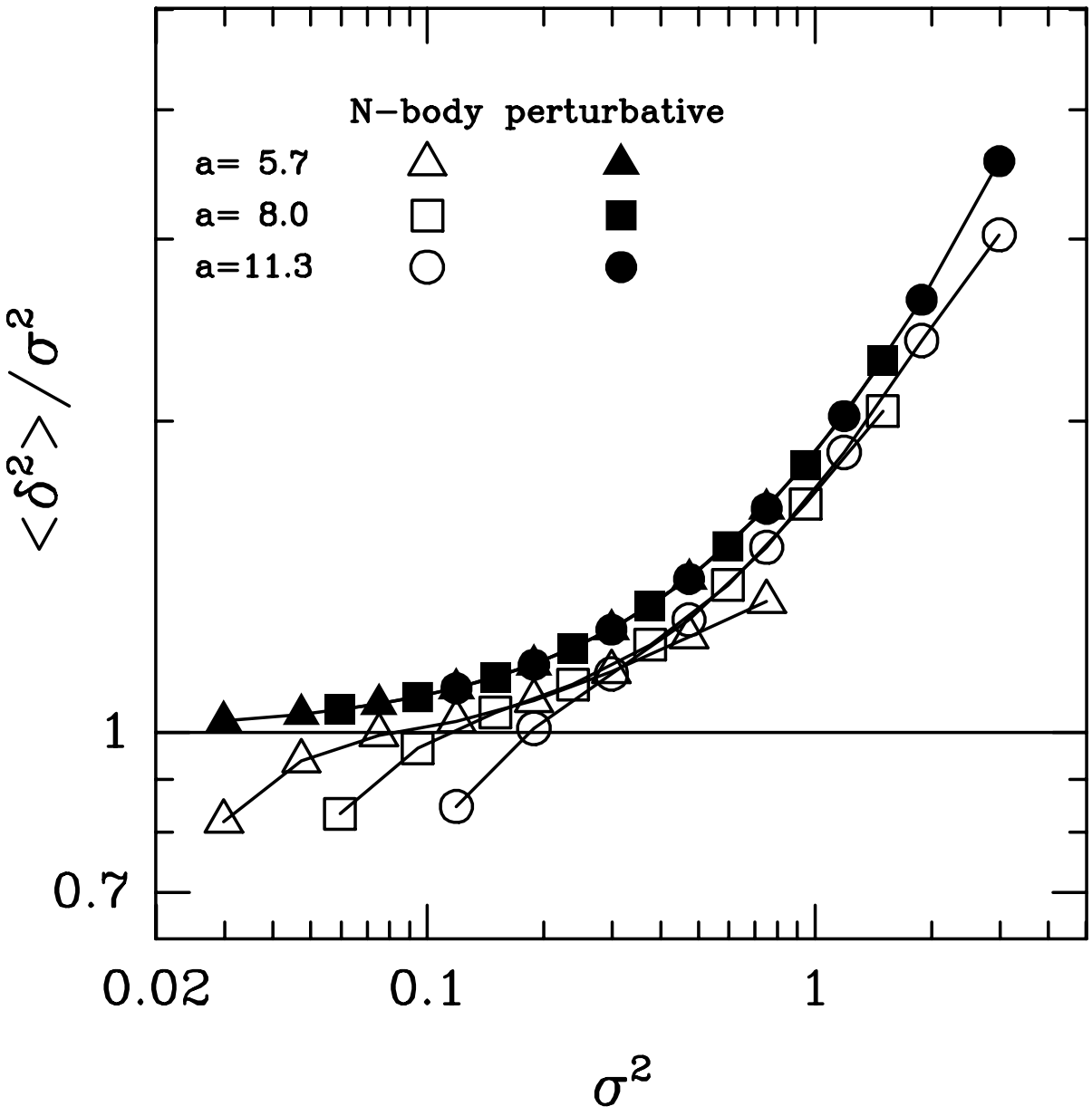
N−body perturbative
a= 5.7
a= 8.0
a=11.3
$<\delta^2>/\sigma^2$
1
0.7
0.02
0.1
1
σ^2

Figure 3

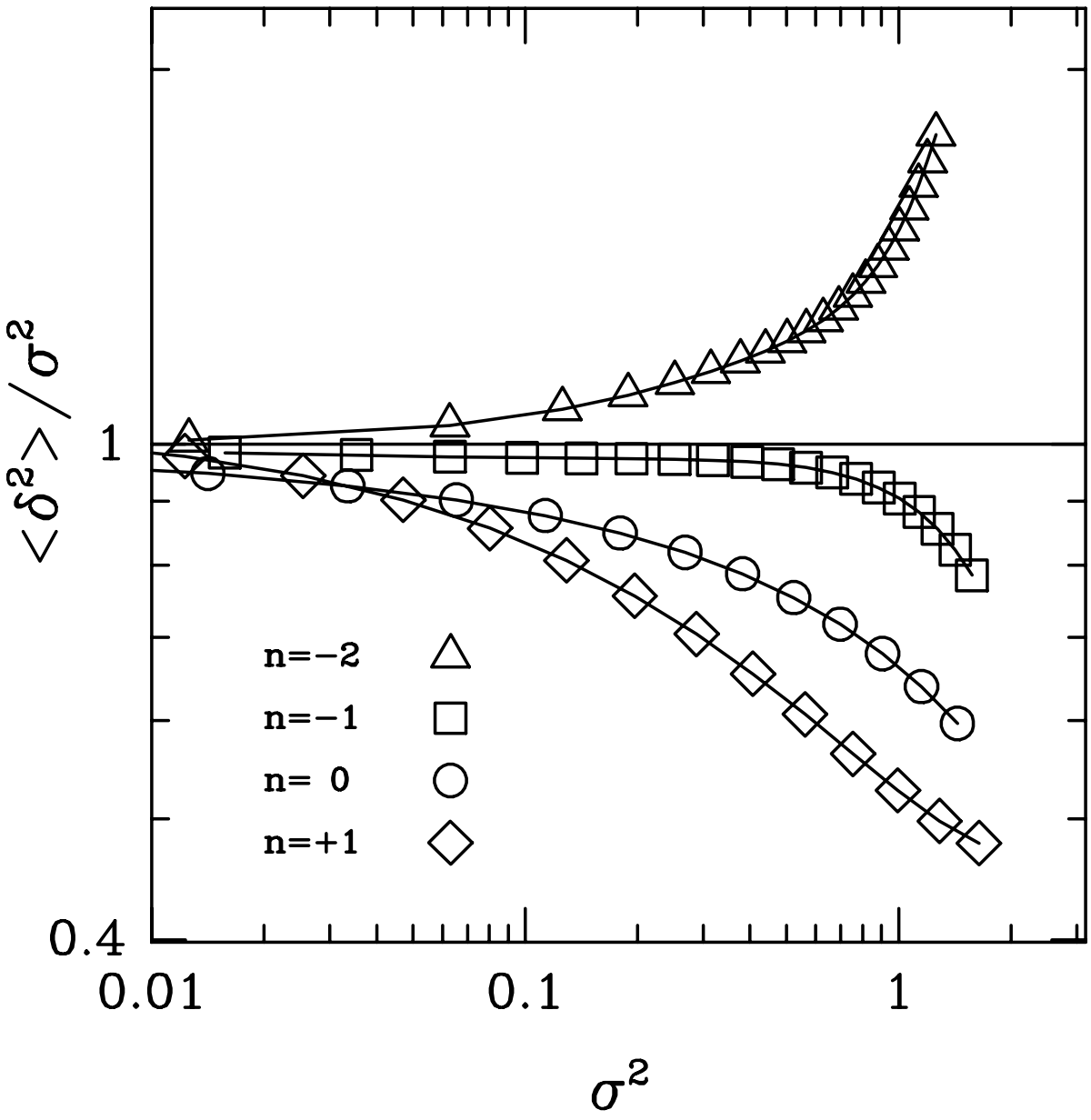

Figure 4